Indonesian Physical Review
Volume 09 Issue 01, January 2026
P-ISSN: 2615-1278, E-ISSN: 2614-7904

Physical Characterization of 3D-Printed HIPS Boluses at Different Thicknesses and Infill Densities for Radiotherapy

Faisal Ahlan Rizaldi[1], Sri Herwiningsih[1*], Dionysius J.D.H. Santjojo[1], Luthfia Aqila Abrar[1]
[1] *Physics Department, Faculty of Mathematics and Natural Science, Brawijaya University, Indonesia.*

Corresponding Authors E-mail: herwin@ub.ac.id

Article Info

Article info:
Received: 26-09-2026
Revised: 01-12-2026
Accepted: 20-12-2026

Keywords:
High-Impact Polystyrene; 3D-Printed Bolus; Relative Electron Density; Radiotherapy

How To Cite:
F.A. Rizaldi, S. Herwiningsih, D.J.D.H. Santjojo, and L.A. Abrar, "Physical Characterization of 3D-Printed HIPS Boluses at Different Thicknesses and Infill Densities for Radiotherapy", Indonesian Physical Review, vol. 9, no. 1, pp 94-106, 2026.

DOI:
https://doi.org/10.29303/ipr.v9i1.583.

Abstract

In external beam radiation therapy, conventional boluses have limitations in conforming to irregular skin surfaces, leading to the formation of air gaps between the skin surface and the bolus. The fabrication of a three-dimensional printed (3D-printed) bolus using 3D printing improves the bolus's conformity to the irregular skin surface. This study aims to evaluate the physical characteristics and tissue-equivalent properties of HIPS filament and 3D-printed HIPS boluses at different thicknesses and infill densities. The physical characteristics of HIPS filament, including density, electron density, and Relative Electron Density (RED), were measured. At the same time, Fourier Transform Infrared (FTIR) spectroscopy was performed to determine the mass fraction percentages of polystyrene and polybutadiene. The 3D-printed HIPS boluses were characterized for bulk density, electron density, RED, water absorption percentage, internal pore size, and total pore volume, with bulk density and RED compared to those of adipose tissue. The physical characteristics of the HIPS filament showed a density of 1.01 g/cm³, an electron density of 3.29 × 10^{23} electrons/cm³, and a RED of 0.98, resembling those of adipose tissue. The physical characteristics of 3D-printed HIPS boluses at different infill densities showed bulk density ranging from 0.61 g/cm³ to 0.81 g/cm³, electron density ranging from 2.00×10^{23} electrons/cm³ to 2.63×10^{23} electrons/cm³, RED ranging from 0.59 to 0.79, and water absorption percentage ranging from 2.9% to 7.9%. The evaluation results showed that the 3D-printed HIPS bolus with a thickness of 0.6 cm and 80% infill density was the optimal configuration, exhibiting the lowest water absorption, smallest internal pore size and total pore volume, with bulk density and RED most similar to those of adipose tissue.

Introduction

Bolus is a tissue-equivalent material commonly used in External Beam Radiotherapy (EBRT) using megavoltage photon or electron beams to increase surface dose, improve the dose distribution to the target, and reduce unnecessary radiation exposure to the underlying tissues [1], [2], [3]. Bolus application is significant for superficial targets where the skin surface is included in the Planning Target Volume (PTV) to counteract the skin-sparing effect [4]. The skin-sparing effect causes the maximum dose to be deposited at a certain depth beneath the skin surface, preventing the skin surface from receiving an adequate dose. The application of a bolus in radiotherapy increases the surface dose by shifting the depth of maximum dose to the skin surface [5].

Conventional boluses are typically fabricated as flat sheets made of silicone rubber, propylene glycol, paraffin wax, natural rubber, or plasticine with various thicknesses [6], [7]. However, conventional bolus has a limited ability to conform to irregular surfaces, creating air gaps between the bolus and the skin [3], [8]. These air gaps cause a dose perturbation that reduces the surface dose and alters the dose distribution to the target [9], [10]. Recent advances in 3D printing technology have enabled the fabrication of patient-specific boluses based on patient CT images, improving the bolus conformity to the irregular surfaces and thereby minimizing air gaps between the bolus and the skin surface [11], [12]. Several hospitals have implemented wax boluses due to their lower fabrication costs compared to commercial boluses [7], [13], [14]. A previous study reported that 3D-printed boluses have a lower fabrication cost than wax boluses. In addition, 3D-printed boluses demonstrated smaller volumetric deviations from the reference virtual bolus plan compared with wax boluses [13].

Previous studies have reported that High-Impact Polystyrene (HIPS) filament is suitable for mimicking adipose tissue due to its radiological characteristics closely resemble those of adipose tissue [15], [16]. Prior studies on 3D-printed HIPS boluses with different thicknesses at 100% infill density demonstrated promising results in shifting 100% of the prescribed dose of both X-ray and electron beams closer to the skin surface [17], [18]. Several studies have examined the performance of 3D-printed boluses at lower infill densities to achieve faster printing times and less filament usage [11], [19]. However, lower infill density decreases both the tissue-equivalent properties and the performance of the 3D-printed bolus in shifting the maximum dose to the skin surface [11], [19], [20]. Nevertheless, a prior study has reported that a 3D-printed Polylactic Acid (PLA) bolus at lower infill density still exhibited acceptable bolus performance and tissue-equivalent properties, while offering faster printing times and reduced filament usage [21].

At lower infill densities, the increased pore size within the bolus facilitates moisture accumulation from ambient air absorbed by the filament, which alters its composition and consequently affects bolus performance and tissue-equivalent properties [20], [22]. This study presents a novel approach to optimizing the thickness and infill density of 3D-printed HIPS bolus, which significantly affect its physical characteristics, including bulk density, electron density, Relative Electron Density (RED), internal pore size, total internal pore volume, and water absorption percentage. Furthermore, the bulk density and RED were compared with those of adipose tissue to evaluate the tissue-equivalent properties of the 3D-printed HIPS bolus. Therefore, this study aims to evaluate the physical characteristics and tissue-equivalent properties of HIPS filament and 3D-printed HIPS boluses at different thicknesses and infill densities.

Experimental Method

Filament Density Test

A 50 cm length of HIPS filament (Indofilam, Bandung, Indonesia) was weighed using a digital scale (Tricle Brand, Shanghai, China), and its diameter was measured using a vernier calliper (Lanter, Shenzhen, China). The density of HIPS filament was calculated using Equation 1 [23]:

$$\rho = \frac{m}{V} \quad (1)$$

Where ρ is the filament's density (g/cm^3), m is the filament's mass (g), and V is the filament's volume (cm) [23]. The calculated density of the HIPS filament was used to calibrate the CreatWare software version 7.2.0 (CreatBot, Zhengzhou, China) and the 3D printer Inova3D i4030 (PT Proinnov Teknologi Indonesia, Tangerang, Indonesia) for slicing and printing with HIPS filament.

Fourier Transform Infrared Spectroscopy (FTIR) Analysis

A HIPS thin plate with dimensions of 2 cm × 2 cm × 0.2 cm was designed using TinkerCad software version 4.3.1 (Autodesk, San Francisco, United States of America). The HIPS thin plate design was imported into CreatWare software, sliced with a rectilinear infill pattern at 100% infill density, and fabricated using a 3D printer Inova3D i4030 and HIPS filament. The printing parameters for fabricating the HIPS thin plate are tabulated in Table 1. These parameters were determined through trial-and-error optimization using HIPS filament. This optimization was performed on a 3D printer Inova i4030 to achieve high print quality while maintaining a short print time.

Table 1. The printing parameters for fabricating the HIPS thin plate and the 3D-printed HIPS bolus

Printing parameters	HIPS thin plate	3D-printed HIPS bolus
Infill pattern	Rectilinear	Gyroid
Top and bottom infill pattern	Rectilinear	Rectilinear
Infill density	100%	20%, 40%, 60%, and 80%
Perimeter wall	2	2
Top layer	5	5
Bottom layer	5	5
Nozzle diameter	0.04 cm	0.04 cm
Layer height	0.04 cm	0.04 cm
Printing speed	4 cm/s	4 cm/s
Nozzle temperature	240°C	240°C
Bed temperature	110°C	110°C

The FTIR measurements were performed on the HIPS thin plate using an IRPrestige-21 spectrometer (Shimadzu Corporation, Kyoto, Japan). The FTIR spectra were analyzed to

determine the mass fraction percentages of polystyrene and polybutadiene in the HIPS filament [24]

Fabrication of 3D-Printed HIPS Boluses

The HIPS boluses were designed in TinkerCAD software as 12 cm × 12 cm plates with thicknesses of 0.6 cm, 0.8 cm, and 1 cm. The HIPS bolus designs were imported into CreatWare software, sliced with a gyroid infill pattern at 20%, 40%, 60%, and 80% infill densities. The HIPS bolus designs were fabricated using a 3D printer Inova i4030, and HIPS filament, with the printing parameters specified in Table 1. In this study, the 3D-printed HIPS boluses with infill densities below 20% were not fabricated due to the formation of large overhanging structures, whereas 3D-printed HIPS boluses with infill densities above 80% were not fabricated due to extreme vibration during fabrication, which caused the infill pattern to overlap with the perimeter wall, leading to wall expansion and decreased dimensional accuracy. The gyroid infill pattern was selected because a previous study on 3D-printed PLA and Thermoplastic Polyurethane (TPU) boluses reported that the gyroid infill pattern produced smaller pore sizes than the rectilinear, cubic, and grid infill patterns, thereby improving the bolus's homogeneity [11].

Water Absorption Percentage Tests

The 3D-printed HIPS boluses with thicknesses of 0.6 cm, 0.8 cm, and 1 cm at 20%, 40%, 60%, and 80% infill densities were weighed using a digital scale. Each bolus was immersed in distilled water in a closed container, with one bolus per container. The entire surface of each bolus was fully immersed in water. After 24 hours of immersion, the 3D-printed HIPS boluses were removed from the container and reweighed on a digital scale. The water absorption percentage of the 3D-printed HIPS bolus was calculated using Equation 2 [25].

$$WA = \frac{m_t - m_0}{m_0} \times 100\% \qquad (2)$$

Where WA is the water absorption percentage (%), m_t is the bolus's mass before immersion (g), and m_0 is the bolus's mass after immersion (g). The water absorption percentage test for the HIPS filament was also performed using the same procedure as applied to the 3D-printed HIPS boluses [25].

Internal Pore Size Measurements

The internal pore structures of 3D-printed HIPS boluses at 20%, 40%, 60%, and 80% infill densities were examined using a Sanwa digital microscope 400-CAM057 (Sanwa Electric Instrument, Tokyo, Japan), captured using a Microsoft Camera software version 2025.2505.2.0 (Microsoft Corporation, Washington, USA), and measured using a Fiji ImageJ software version 1.8.0_322 (National Institutes of Health, Maryland, USA). The total internal pore volume of the 3D-printed HIPS boluses was calculated using CreatWare software by subtracting the bulk volume and the actual volume. The bulk volume represents the total volume of the bolus, including internal pore volume. In contrast, the actual volume represents only the total volume of the solid material bolus, excluding internal pore volume [26].

RED Calculation of 3D-Printed HIPS Boluses

The electron density of 3D-printed HIPS boluses at 20%, 40%, 60%, and 80% infill densities was calculated using the Shrimpton Equation as expressed in Equation 3. In contrast, the RED

of the 3D-printed HIPS bolus was calculated using Equation 4. The RED of 3D-printed HIPS boluses at different infill densities was compared with the RED of adipose tissue [16].

$$\rho_{e,m} = \rho_m N_A \left(\sum w_i \left(\frac{Z}{A} \right)_i \right)_m \quad (3)$$

$$RED = \frac{\rho_{e,m}}{\rho_{e,w}} \quad (4)$$

Where RED is the relative electron density, $\rho_{e,m}$ is the electron density of bolus (electrons/cm^3), $\rho_{e,w}$ is the electron density of water (electrons/cm^3), ρ_m is the density of bolus (g/cm^3), Z is the atomic number, A is the atomic mass (amu), N_A is Avogadro's constant (6.022×10^{23} mol^{-1}), and w is the mass fraction percentage (%). The subscripts of m and w refer to the 3D-printed HIPS bolus and water, respectively. [16]. The subscript i denotes the elemental compositions of the 3D-printed HIPS bolus, which consists of polystyrene, polybutadiene, and air. The element data for Z and A were obtained from Pacific Northwest National Laboratory (PNNL) [27].

The 3D-printed boluses with infill densities below 100% contained internal pores filled with air, and consequently, the w_i values for 3D-printed HIPS bolus included contributions from both HIPS filament and air. The elemental compositions of air and their mass fraction percentages were obtained from the standard atmospheric composition [28]. The HIPS filament itself consisted of polystyrene and polybutadiene. The mass fraction percentages of polystyrene and polybutadiene in the HIPS filament were determined from FTIR spectra. In contrast, the mass fraction percentages of HIPS filament and air in the 3D-printed boluses were determined from each bolus' infill density. These values were used to calculate the overall mass fraction percentages of polystyrene, polybutadiene, and air in the 3D-printed HIPS bolus at each infill density [24].

Result and Discussion

Physical Characteristics of HIPS Filament

The bolus material should closely resemble the physical characteristics of human tissue to ensure that the atomic constituent characteristics of the bolus resemble those of human tissue [16]. The physical characteristics of HIPS filament and adipose tissue are summarized in Table 2.

Table 2. Physical characteristics of HIPS filament and adipose tissue.

Physical characteristics	HIPS filament	Adipose tissue [29]	Relative difference (%)
Density (g/cm^3)	1.01	0.94	7.45
Electron density ($electrons/cm^3$)	3.29×10^{23}	3.11×10^{23}	5.79
RED	0.98	0.93	5.38

Table 2 shows that the relative differences in electron density and RED between the HIPS filament and adipose tissue were 5.79% and 5.38%, respectively. Since electron density is the primary determinant of photon and electron interactions in tissue, these findings indicate that

the HIPS filament is suitable for mimicking adipose [30]. Table 3 presents the water absorption percentage and HIPS filament composition.

Table 3. Water absorption percentage and HIPS filament compositions

Parameters	HIPS filament
Water absorption percentage (%)	0.98
Polystyrene content (%)	97
Polybutadiene content (%)	3.0

Table 3 shows that HIPS filament absorbs little water from a humid environment, indicating that it is less hygroscopic. The HIPS filament was composed of 97% polystyrene (C_8H_8) and 3% polybutadiene (C_4H_6), with hydrogen as the most abundant atomic constituent, followed by carbon. Similarly, adipose tissue is composed of hydrogen (63%), carbon (28%), and oxygen (7.7%), with hydrogen as the most abundant constituent, followed by carbon and oxygen. The similarity in atomic composition indicated that the HIPS filament is suitable for mimicking adipose tissue [27].

Physical Characteristics of 3D-Printed HIPS Bolus

Infill density represents the total amount of HIPS filament deposited within the 3D-printed HIPS bolus, which affects the bolus's density [31]. Table 4 shows the bulk density, electron density, RED, and internal pore size of 3D-printed HIPS boluses at different infill densities.

Table 4. Bulk density and electron density of 3D-printed HIPS boluses at different infill densities.

Infill density (%)	Bulk density (g/cm^3)	Electron density ($electrons/cm^3$)	RED	Internal pore size (cm)
20	0.61	2.00×10^{23}	0.60	0.26
40	0.66	2.14×10^{23}	0.65	0.08
60	0.74	2.40×10^{23}	0.73	0.04
80	0.81	2.63×10^{23}	0.80	0.02

Table 4 shows that a lower infill density decreased the bulk density, electron density, and RED of the 3D-printed HIPS bolus. This is because a lower infill density reduced the total amount of HIPS filament deposited within the bolus, leading to fewer HIPS atomic constituents per unit volume [31]. As a result, the bulk density, electron density, and RED of the 3D-printed HIPS bolus decreased. These findings are similar to previous studies on 3D-printed HIPS phantom with grid, concentric, honeycomb, lines, and triangles infill patterns at different infill densities, where reducing infill density led to lower RED [32]. Although the previous study used a different infill pattern and calculated RED by converting Hounsfield Units (HU) rather than using the Shrimpton equation, the RED of 3D-printed HIPS reported in that study was

similar to the RED obtained in this study, with slightly higher values in this study due to the use of a gyroid infill pattern [32].

A previous study on 3D-printed PLA and TPU boluses reported that the gyroid infill pattern produced smaller internal pore sizes compared with rectilinear, grid, and cubic infill patterns [11]. Smaller internal pore size results in a denser bolus's density, which increases the electron density and RED of the bolus [11]. Figure 1 shows the internal pore structure of 3D-printed HIPS boluses with a gyroid infill pattern at different infill densities.

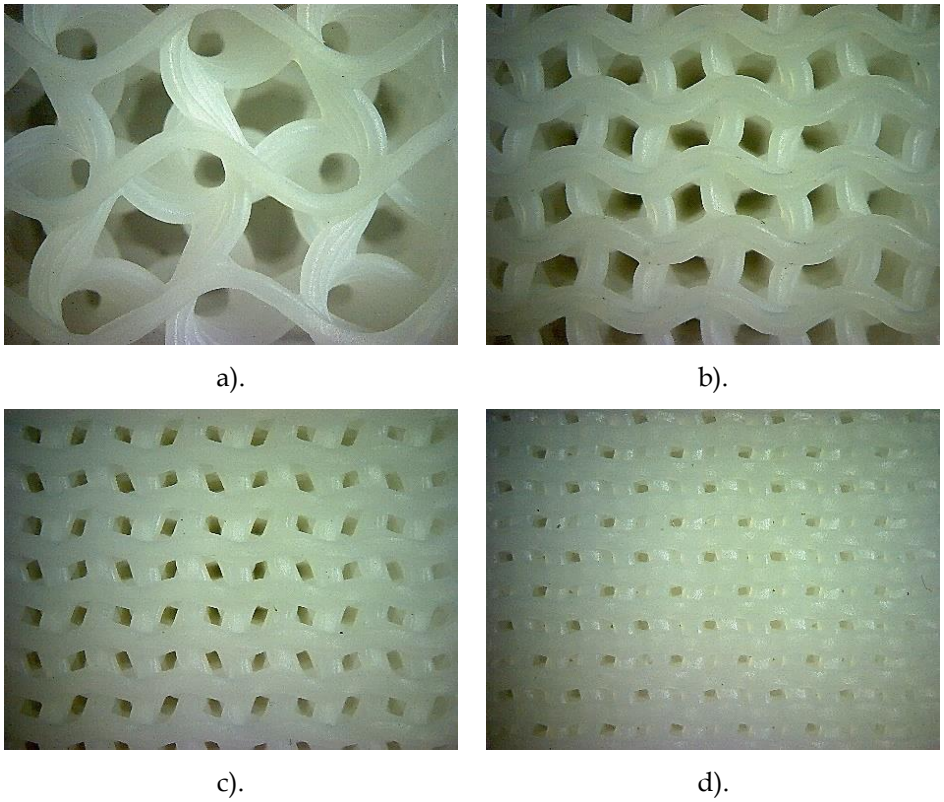

Figure 1. Internal pore structure of 3D-printed HIPS boluses a). 20% infill density, b). 40% infill density, c). 60% infill density, and d). 80% infill density

Figure 1 shows that a lower infill density resulted in less HIPS filament deposited within the bolus, leaving more void volume, which increased the internal pore size and made the bolus less homogeneous. In contrast, higher infill density resulted in more HIPS filament deposited within the bolus, ensuring more void volume could be filled with HIPS filament and leaving less void volume, thereby decreasing the internal pore size and making the bolus more homogeneous. These findings are consistent with a previous study on 3D-printed PLA and TPU boluses with honeycomb infill pattern, which reported that reducing infill density increased the internal pore size [20]. Figure 2 shows the total internal pore volume of 3D-printed HIPS boluses at different thicknesses and infill densities.

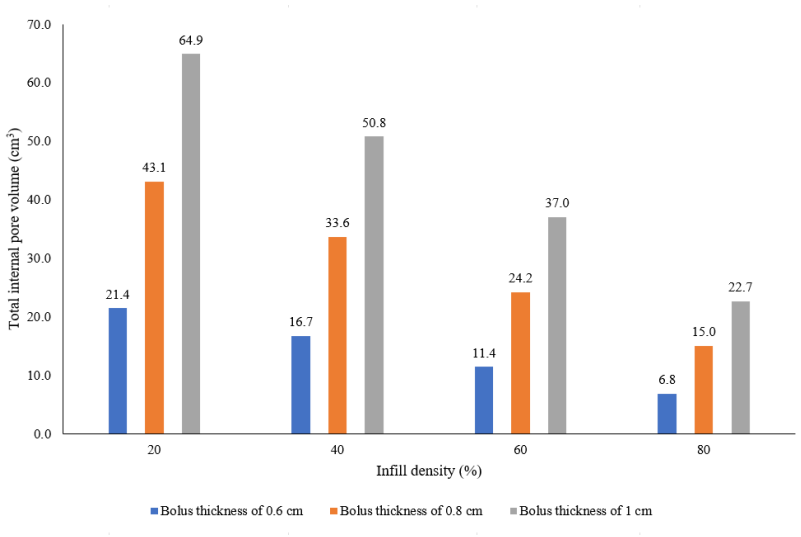

Figure 2. The total internal pore volume of 3D-printed HIPS boluses at different thicknesses and infill densities.

Figure 2 shows that a thicker bolus and a lower infill density resulted in a larger total internal pore volume. This occurs because increasing the bolus's thickness enlarges the overall bolus volume, thereby increasing the number of internal pores, leading to a larger total internal pore volume. In addition, decreasing the bolus's infill density led to larger internal pores, thereby increasing the total internal pore volume. Figure 3 presents the water absorption percentage of 3D-printed HIPS boluses at different thicknesses and infill densities.

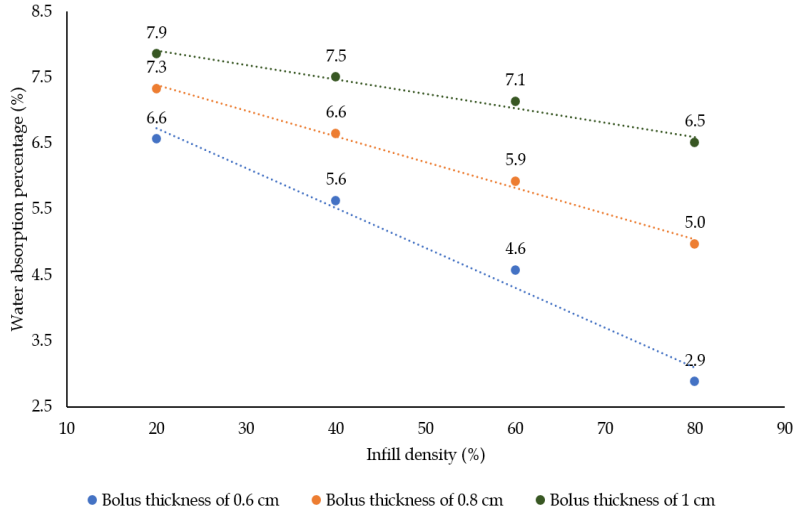

Figure 3. Water absorption percentages of 3D-printed HIPS boluses at different thicknesses and infill densities.

Figure 3 shows that a thicker bolus and lower infill density resulted in a higher water absorption percentage. This is because a thicker bolus and lower infill density led to a larger internal pore size, increasing the amount of water that could be accumulated within the bolus's

pores. It should be noted that in this study, the printing parameters, including perimeter wall, top layer, bottom layer, nozzle diameter, and layer height, were kept constant. These parameters form structural boundaries between the external environment and the internal pores, thereby influencing water penetration into the internal pores [33]. Further research is needed to evaluate the effects of variations in these printing parameters on the water absorption percentage of 3D-printed HIPS boluses.

Tissue-Equivalent Properties of 3D-Printed HIPS Bolus.

The tissue-equivalent properties of 3D-printed HIPS boluses were evaluated by comparing their bulk density and RED with those of adipose tissue [16]. Tables 5 and 6 present the relative differences in bulk density and RED between 3D-printed HIPS boluses at different infill densities and adipose tissue.

Table 5. The relative difference in bulk density between the 3D-printed HIPS bolus and adipose tissue**.**

Infill density (%)	Bulk density (g/cm³)		Relative difference (%)
	3D-printed HIPS Bolus	Adipose tissue [29]	
20	0.60	0.94	36.2
40	0.65		30.8
60	0.73		22.3
80	0.80		14.9

Table 6. The relative difference in RED between the 3D-printed HIPS bolus and adipose tissue**.**

Infill density (%)	RED		Relative difference (%)
	3D-printed HIPS Bolus	Adipose tissue [29]	
20	0.59	0.93	36.6
40	0.64		31.2
60	0.72		22.6
80	0.79		15.1

As shown in Tables 5 and 6, boluses with higher infill density showed minor relative differences in bulk density and RED compared to adipose tissue, indicating that 3D-printed HIPS boluses at higher infill density more closely mimic adipose tissue. This is because a higher infill density decreases the internal pore size and, consequently, increases the bolus's homogeneity, making it more closely resemble soft tissue [31].

The 3D-printed HIPS boluses with thicknesses of 0.6 cm at 60% and 80% infill densities, as well as the 3D-printed HIPS bolus with a thickness of 0.8 cm at 80% infill density, demonstrated

water absorption below 5%. However, as shown in Figure 2, the 3D-printed HIPS bolus with a thickness of 0.6 cm had a smaller total internal pore volume compared to the 3D-printed HIPS bolus with a thickness of 0.8 cm. The 3D-printed HIPS boluses at 80% infill density showed bulk density, electron density, and RED that most closely resembled those of adipose tissue. Furthermore, the 3D-printed HIPS bolus at 80% infill density demonstrated the most homogeneous internal pore structure, the smallest pore size, and the smallest total internal pore volume. Therefore, based on the evaluation of physical characteristics, the best configuration of a 3D-printed HIPS bolus was 0.6 cm thickness at 80% infill density. Nevertheless, further studies are required to evaluate the radiological and dosimetric characteristics of 3D-printed HIPS boluses at different thicknesses and infill densities.

Conclusion

HIPS filament is less hygroscopic. In addition, HIPS filament demonstrated electron density, and RED closely resembled those of adipose tissue. Higher infill density increased bulk density, electron density, and RED, thereby more closely resembling adipose tissue. The thinner bolus and higher infill density decreased total internal pore volume and water absorption percentage. A 3D-printed HIPS bolus with a 0.6 cm thickness at 80% infill density was identified as the best configuration of bolus thickness and infill density. This finding demonstrates the potential use of 3D-printed HIPS as a radiotherapy bolus. Future work should evaluate the radiological and dosimetric characteristics of 3D-printed HIPS boluses.

Acknowledgment

The authors thank Prof. Dr. Unggul Punjung Juswono, S.Si., M.Sc., and Prof. Chomsin Sulistya Widodo, S.Si., M.Si., Ph.D., for their suggestions and support in completing this study.

References

[1] D. Kong *et al.*, "Effect of bolus materials on dose deposition in deep tissues during electron beam radiotherapy," *J Radiat Res*, vol. 65, no. 2, pp. 215–222, Mar. 2024.

[2] X. Wang *et al.*, "3D-printed bolus ensures the precise postmastectomy chest wall radiation therapy for breast cancer," *Front Oncol*, vol. 12, Sep. 2022

[3] Y. Zhang *et al.*, "A clinical trial to compare a 3D-printed bolus with a conventional bolus with the aim of reducing cardiopulmonary exposure in postmastectomy patients with volumetric modulated arc therapy," *Cancer Med*, vol. 11, no. 4, pp. 1037–1047, Feb. 2022.

[4] S. Herwiningsih *et al.*, "Radiation Therapy (3DCRT) Breast Cancer Treatment Plans," *Indonesian Physical Review*, vol. 6, no. 3, pp. 284–293, 2023.

[5] F. Li, W. Hu, H. Li, B. Li, and Y. Wang, "Bolus Use in Postmastectomy Radiation Therapy for Breast Cancer: A Systematic Literature Review," *Technol Cancer Res Treat*, vol. 24, Jan. 2025.

[6] A. P. Hariyanto, F. U. Mariyam, L. Almira, E. Endarko, and B. H. Suhartono, "Fabrication and characterization of bolus material using propylene glycol for radiation therapy," *Iranian Journal of Medical Physics*, vol. 17, no. 3, pp. 161–169, 2020.

[7] E. Endarko, S. Aisyah, C. C. C. Carina, T. Nazara, G. Sekartaji, and A. Nainggolan, "Evaluation of dosimetric properties of handmade bolus for megavoltage electron and photon radiation therapy," *J Biomed Phys Eng*, vol. 11, no. 6, pp. 735–746, Dec. 2021.

[8] J. L. Robar *et al.*, "Intrapatient study comparing 3D printed bolus versus standard vinyl gel sheet bolus for postmastectomy chest wall radiation therapy," *Pract Radiat Oncol*, vol. 8, no. 4, pp. 221–229, Jul. 2018.

[9] L. Dilson *et al.*, "Estimation of Surface Dose in the Presence of Unwanted Air Gaps under the Bolus in Postmastectomy Radiation Therapy: A Phantom Dosimetric Study," *Asian Pacific Journal of Cancer Prevention*, vol. 23, no. 9, pp. 2973–2981, 2022.

[10] D. Lobo, C. Srinivas, S. Banerjee, M. S. Athiyamaan, K. Johan Sunny, and A. Krishna, "Estimation of surface doses in the presence of an air gap under a bolus for a 6 MV clinical photon beam - a phantom study," *Radiat Environ Biophys*, vol. 64, no. 1, pp. 77–83, Mar. 2025.

[11] S. G. Gugliandolo *et al.*, "3D-printed boluses for radiotherapy: influence of geometrical and printing parameters on dosimetric characterization and air gap evaluation," *Radiol Phys Technol*, vol. 17, no. 2, pp. 347–359, Jun. 2024.

[12] D. Basaula *et al.*, "Additive manufacturing of patient specific bolus for radiotherapy: large scale production and quality assurance," *Phys Eng Sci Med*, vol. 47, no. 2, pp. 551–561, Jun. 2024.

[13] C. Albantow, C. Hargrave, A. Brown, and C. Halsall, "Comparison of 3D printed nose bolus to traditional wax bolus for cost-effectiveness, volumetric accuracy and dosimetric effect," *J Med Radiat Sci*, vol. 67, no. 1, pp. 54–63, Mar. 2020.

[14] B. Ananthi, K. Bhuvana, R. Faith, G. Selvaluxmy, N. Vivekanandan, and I. Priya, "Conformal electron beam radiotherapy using custom-made step bolus for postmastectomy chest wall irradiation: An institutional experience," *J Cancer Res Ther*, vol. 15, no. 5, pp. 999–1004, Jul. 2019.

[15] X. Ma, M. Figl, E. Unger, M. Buschmann, and P. Homolka, "X-ray attenuation of bone, soft and adipose tissue in CT from 70 to 140 kV and comparison with 3D printable additive manufacturing materials," *Sci Rep*, vol. 12, no. 1, Dec. 2022.

[16] M. Bento *et al.*, "Characterisation of 3D-printable thermoplastics to be used as tissue-equivalent materials in photon and proton beam radiotherapy end-to-end quality assurance devices," *Biomed Phys Eng Express*, vol. 10, no. 6, Nov. 2024.

[17] K. H. Jung, D. H. Han, K. Y. Lee, J. O. Kim, W. S. Ahn, and C. H. Baek, "Evaluating the performance of thermoplastic 3D bolus used in radiation therapy," *Applied Radiation and Isotopes*, vol. 209, Jul. 2024.

[18] D. H. Han *et al.*, "Dosimetric Characteristics of a 3D-printed Bolus Fabricated using Different Filament Materials for Radiation Therapy," *New Physics: Sae Mulli*, vol. 72, no. 10, pp. 806–811, Oct. 2022.

[19] R. Ricotti *et al.*, "Dosimetric characterization of 3D printed bolus at different infill percentage for external photon beam radiotherapy," *Physica Medica*, vol. 39, pp. 25–32, Jul. 2017.

[20] E. Dąbrowska-Szewczyk *et al.*, "Low-density 3D-printed boluses with honeycomb infill 3D-printed boluses in radiotherapy," *Physica Medica*, vol. 110, Jun. 2023.

[21] A. Yuliandari, S. Oktamuliani, Harmadi, and F. Diyona, "Dosimetric Characterization of 3D Printed Bolus with Polylactic Acid (PLA) in Breast Cancer External Beam Radiotherapy," *Iranian Journal of Medical Physics*, vol. 21, no. 3, pp. 211–216, 2024.

[22] B. Ergene, Y. E. İnci, B. Çetintaş, and B. Daysal, "An experimental study on the wear performance of 3D printed polylactic acid and carbon fiber reinforced polylactic acid parts: Effect of infill rate and water absorption time," *Polym Compos*, vol. 46, no. 1, pp. 372–386, Jan. 2025.

[23] M. Boopathi, D. Khanna, P. Venkatraman, R. Varshini, C. S. Sureka, and S. Pooja, "Fabrication and Dosimetric Characteristics of Silicon Elastomer-Based Bolus Using External Beam Radiotherapy," *Asian Pacific Journal of Cancer Prevention*, vol. 24, no. 1, pp. 141–147, 2023.

[24] N. S. Giakoumakis *et al.*, "Total revalorization of high impact polystyrene (HIPS): enhancing styrene recovery and upcycling of the rubber phase," *Green Chemistry*, vol. 26, no. 1, pp. 340–352, Nov. 2023.

[25] ASTM, "ASTM D570-22 : Standard Test Method for Water Absorption of Plastics," ASTM International, West Conshohocken, PA, Sep. 2022.

[26] I. Buj-Corral, A. Bagheri, A. Dominguez-Fernandez, and R. Casado-Lopez, "Influence of infill and nozzle diameter on porosity of FDM printed part with rectilinear grid pattern," *Procedia Manuf*, vol. 41, pp. 288–5, 2019.

[27] PNNL, "Data Mining Analysis and Modeling Cell Compendium of Material Composition Data for Radiation Transport Modeling," Washington, 2021.

[28] O. Rusoke-Dierich, "Composition of The Normal Air," *in Diving Medicine*, Cham: Springer, 2018, ch. 6, pp. 41–42.

[29] K. Usui, K. Ogawa, and K. Sasai, "Analysis of Dose Calculation Accuracy in Cone Beam Computed Tomography with Various Amount of Scattered Photon Contamination," *Int J Med Phys Clin Eng Radiat Oncol*, vol. 06, no. 03, pp. 233–251, 2017.

[30] F. M. Khan, "Dose Distribution and Scatter Analysis," *in The Physics of Radiation Therapy*, 3rd ed., Philadelphia: Lippincott Williams & Wilkins, 2003, ch. 9, pp. 159–177.

[31] M. Q. dos Reis, R. J. C. Carbas, E. A. S. Marques, and L. F. M. da Silva, "Effect of the Infill Density on 3D-Printed Geometrically Graded Impact Attenuators," *Polymers (Basel)*, vol. 16, no. 22, Nov. 2024.

[32] J. Madamesila, P. McGeachy, J. E. Villarreal Barajas, and R. Khan, "Characterizing 3D printing in the fabrication of variable density phantoms for quality assurance of radiotherapy," *Physica Medica*, vol. 32, no. 1, pp. 242–247, Jan. 2016.

[33] H. Bakhtiari, M. Nikzad, and M. Tolouei-Rad, "Influence of Three-Dimensional Printing Parameters on Compressive Properties and Surface Smoothness of Polylactic Acid Specimens," *Polymers (Basel)*, vol. 15, no. 18, Sep. 2023.